

## **Effect of Trace Concentrations of H<sub>2</sub>S Introduced to Existing Sweet Corrosion Product Layers**

Adam Cutright, Bruce Brown, David Young  
Institute for Corrosion and Multiphase Technology  
342 West State Street  
Athens, Ohio, 45701  
United States

### **ABSTRACT**

Simulation of reservoir souring has been a neglected area of corrosion research. The procedure followed herein is to form a sweet corrosion product layer, introduce a low concentration of H<sub>2</sub>S in the gas phase (<100ppm) and allow the system to continue to evolve. The experimental apparatus used was a 2L glass cell with an impeller in the center and 5 samples spaced evenly around it to allow for *in situ* corrosion rate monitoring and extraction of specimens for surface analysis. In experiments involving Fe<sub>3</sub>C residues the general corrosion rate decreased when H<sub>2</sub>S was added to the system. FeS was detected on the samples with the Fe<sub>3</sub>C; it is postulated that a thin layer of FeS forms leading to the decrease in general corrosion rate. When the FeCO<sub>3</sub> was challenged with H<sub>2</sub>S, the general corrosion rate increased. FeS was detected on the samples, but no significant change was observed in the FeCO<sub>3</sub>. However, it was electrochemically determined that the H<sub>2</sub>S impacted the FeCO<sub>3</sub> sufficiently to allow the general corrosion rate to increase.

Key words: Corrosion mechanisms, Corrosion rate, Hydrogen Sulfide, Oil and gas, Carbon dioxide

### **INTRODUCTION**

A 2002 study estimated the annual cost associated with corrosion of gas pipelines to be around \$5 billion.<sup>1</sup> Corrosion of oil and gas pipelines continues to pose a major issue in the oil and gas industry due to the combination of brine produced with the oil and the type of acid gas present which can lead to significant internal corrosion. Oil and gas reservoirs can be separated into two categories, sweet and sour. In sweet reservoirs carbon dioxide (CO<sub>2</sub>) is the dominant gas species that dissolves in the brine and hydrates to form carbonic acid which can increase the corrosion rate through a buffering effect but can also dissociate to react with ferrous ions to form corrosion product layers containing iron carbonate in the iron carbide matrix of the mild steel pipeline material. In sour reservoirs hydrogen sulfide (H<sub>2</sub>S) is the dominant corrosive gas species, which similarly will dissolve in the brine and react with ferrous ions to form iron sulfide corrosion product layers associated with its presence, such as mackinawite. Understanding the characteristics of a reservoir is essential when planning how to appropriately mitigate the corrosion that

may occur, which includes material selection, inhibitor selection, and many other strategies. However, if a reservoir changes from sweet to sour, this can cause a large problem as the strategies previously selected and implemented may no longer be sufficient to control the corrosion. When H<sub>2</sub>S begins to appear in a previously sweet reservoir, this is a phenomenon commonly known as souring. This can come about from a variety of pathways, the two most common being souring due to the presence of sulfate reducing bacteria (SRB) being unintentionally injected into the reservoir which then begin to produce H<sub>2</sub>S. It is also possible that the SRB may already be present in the reservoir, but the injection water used may contain a high concentration of sulfate which then leads to the formation of H<sub>2</sub>S. Regardless of how the reservoir begins to sour, it is important to understand what changes may occur once the souring has begun.

At the onset of souring the concentration of H<sub>2</sub>S may remain relatively low for a significant period of time, meaning that the system will likely have whatever corrosion product layers had formed in the sweet corrosion system, being exposed to small concentrations of H<sub>2</sub>S. Previous work has aimed at understanding the impact of low concentrations of H<sub>2</sub>S in CO<sub>2</sub> systems, finding that the general corrosion rate decreases.<sup>2,3</sup> Previous work has also shown that, under highly saturated conditions for iron carbonate and iron sulfide in a system containing both CO<sub>2</sub> and H<sub>2</sub>S, it is possible to form a mixed layer. This same work also showed that under these conditions, the iron carbonate that was originally present as part of the corrosion product layer may disappear over time, which can be seen in the comparison of an X65 steel after a 1 hour exposure (Figure 1) and a 24 hour exposure (Figure 2).<sup>4</sup>

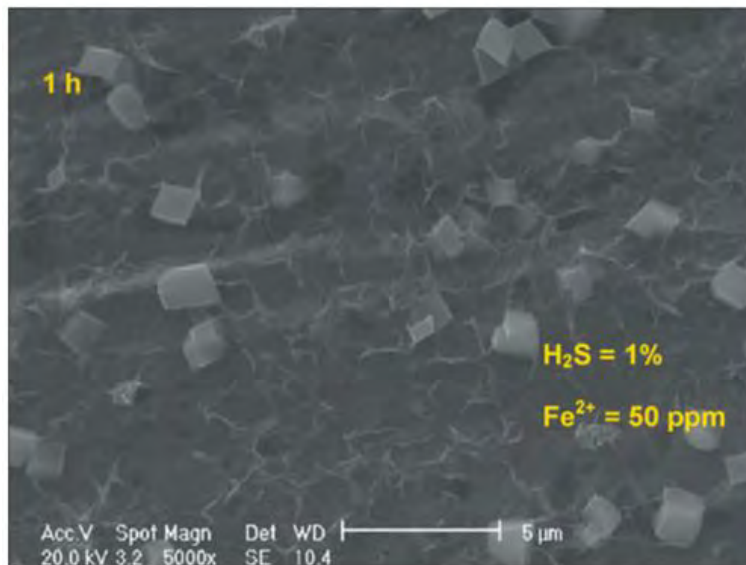


**Figure 1. Mixed FeS and FeCO<sub>3</sub> layer in 1% H<sub>2</sub>S with 50 ppm Fe<sup>2+</sup> at 80°C, pH 6.6±0.05, 1 hour exposure.<sup>4</sup>**

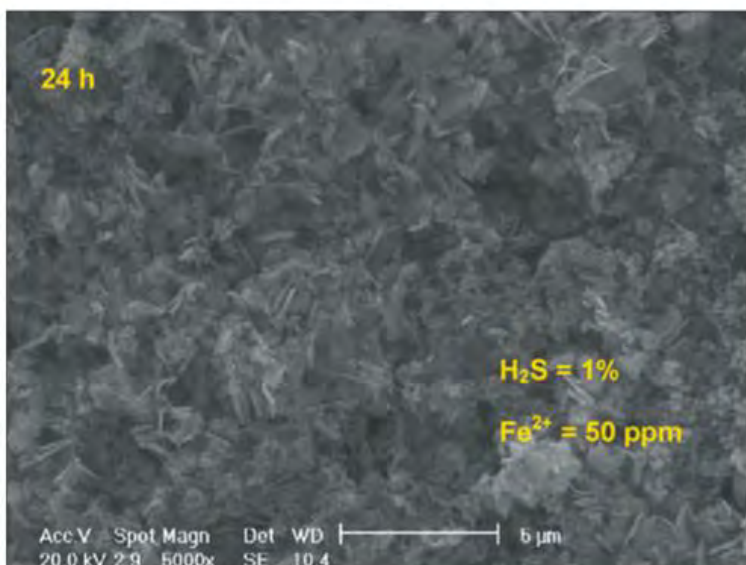


**Figure 2. FeS layer in 1% H<sub>2</sub>S with 50 ppm Fe<sup>2+</sup> at 80°C, pH 6.6±0.05, 24 hour exposure.**<sup>4</sup>

In Figure 1, iron carbonate crystals were precipitated on top of an iron sulfide layer that had formed within a 1-hour exposure time. However, in Figure 2, a sample from the same system extracted after 24 hours exposure shows only iron sulfide.

## EXPERIMENTAL PROCEDURE

Experiments were conducted in a 2L glass cell filled with 1 wt% NaCl with 5 samples placed evenly around a central impeller allowing for similar flow conditions on all 5 samples, the glass cell setup can be seen below in Figure 3. Of the 5 samples present, one was capable of in-situ electrochemical measurements in conjunction with a Ag/AgCl reference electrode connected via Luggin capillary and a platinum coated mesh serving as the counter electrode. Two different sets of conditions were used in the data provided, in one the test cell was maintained at 1 bar, 30°C, and pH 4.0±0.05, and in the other the test cell was maintained at 1 bar, 80°C, and pH 6.6±0.05. The impeller, when used, was fixed at 75 rpm which provides flow properties to the samples similar to 1 m/s in a pipe with an inner diameter of 10 cm.

The results presented here involve experiments which can be separated into two stages. The first stage consists of the formation of a sweet corrosion product layer in the presence of pure CO<sub>2</sub>, and in the second stage trace concentrations of H<sub>2</sub>S will be introduced into the sparge gas. At the start of each experiment the glass cell setup would be sparged with pure CO<sub>2</sub> to remove oxygen from the glass cell. Solutions of hydrochloric acid or sodium bicarbonate would be used to adjust the pH to the desired value. The X65 metal samples would be polished using 600 grit SiC paper until no polishing marks were visible on the sample surface. The composition of the X65 steel can be seen below in Table 1. Once the samples were inserted into the system the desired iron carbonate corrosion product layer would be formed, then a sample would be extracted for analysis immediately prior to the introduction of the H<sub>2</sub>S to have a baseline layer condition for comparison. Additional samples would be extracted throughout the exposure to H<sub>2</sub>S to understand the development or changes in the corrosion product layer over time. The electrochemical sample would be used to take periodic linear polarization resistance (LPR) measurements to have an *in-situ* measurement of the general corrosion rate, as well as electrochemical impedance spectroscopy (EIS) measurements to determine solution resistance.

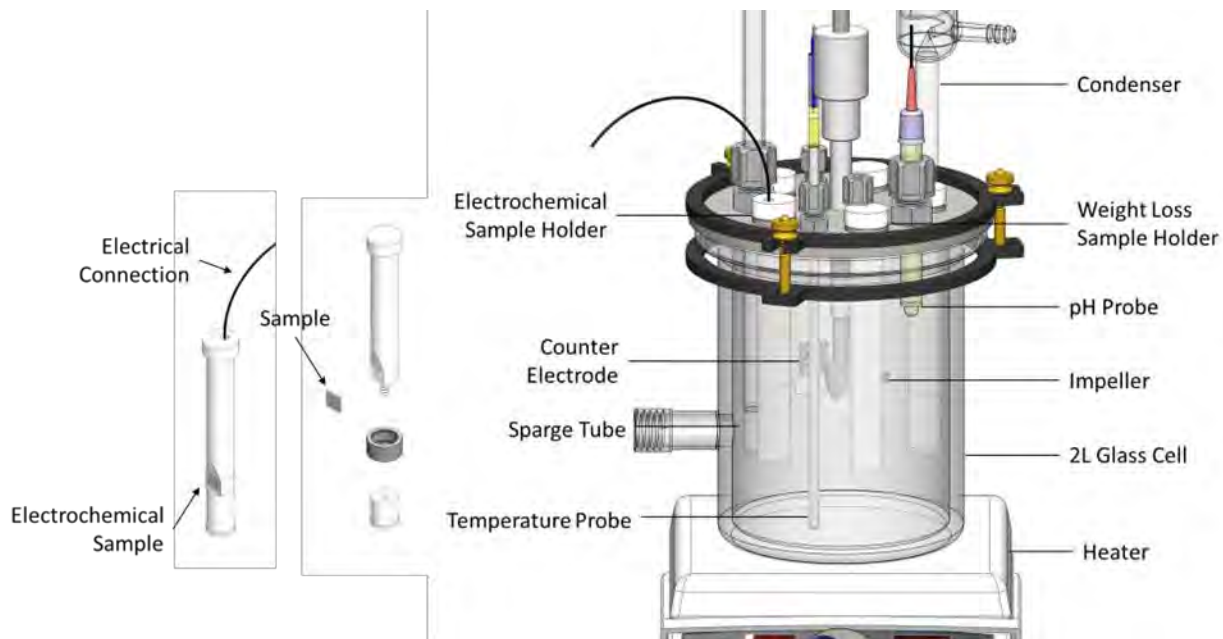


Figure 3. Glass cell setup used during experimentation.

Table 1. X65 steel composition

C	Mn	Nb	Si	V	Mo	Cu	Cr	Ni	Fe
0.05%	1.40%	0.04%	0.22%	0.03%	0.07%	0.11%	0.23%	0.24%	97.52%

Table 2. Experimental conditions

Parameter	Fe <sub>3</sub> C Experiment	FeCO <sub>3</sub> Experiment
Temperature	30°C (86°F)	80°C (176°F)
pH	4.00±0.05	6.60±0.05
Total pressure	1.01 bar (14.7 psi)	1.01 bar (14.7 psi)
Electrolyte	1 wt% NaCl	1 wt% NaCl
Impeller speed	75 rpm	0, 75 rpm
Equivalent pipe velocity	1 m/s (3.3 ft/s)	0, 1 m/s (3.3 ft/s)
Specimen	X65 steel	X65 steel
Gas phase components	CO <sub>2</sub> and H <sub>2</sub> S	CO <sub>2</sub> and H <sub>2</sub> S
Electrochemical methods	LPR, EIS	LPR, EIS
H <sub>2</sub> S <sub>(g)</sub> concentration	60 ppm	80 ppm
Layer formation time	72 hours	48 hours
Total test time	144 hours	114 hours

## EXPERIMENTAL RESULTS

### Exposure of an iron carbide layer (Fe<sub>3</sub>C) to slightly sour environment

First, testing conducted to first form an iron carbide layer before the introduction of H<sub>2</sub>S will be reviewed, the conditions for the formation can be found in Table 2 (Fe<sub>3</sub>C Experiment). The iron carbide layer was formed over 72 hours in pure CO<sub>2</sub> saturated solution at pH 4.0±0.05 and 30°C with an impeller speed of 75 rpm. After the formation of the iron carbide layer, 60 ppm H<sub>2</sub>S in the gas phase was introduced to the system, all other parameters remained constant. The experiment continued with the 60 ppm H<sub>2</sub>S for a further 72 hours before the experiment was concluded. The corrosion rate obtained from the *in situ* LPR measurements over the duration of the experiment can be seen below in Figure 4.

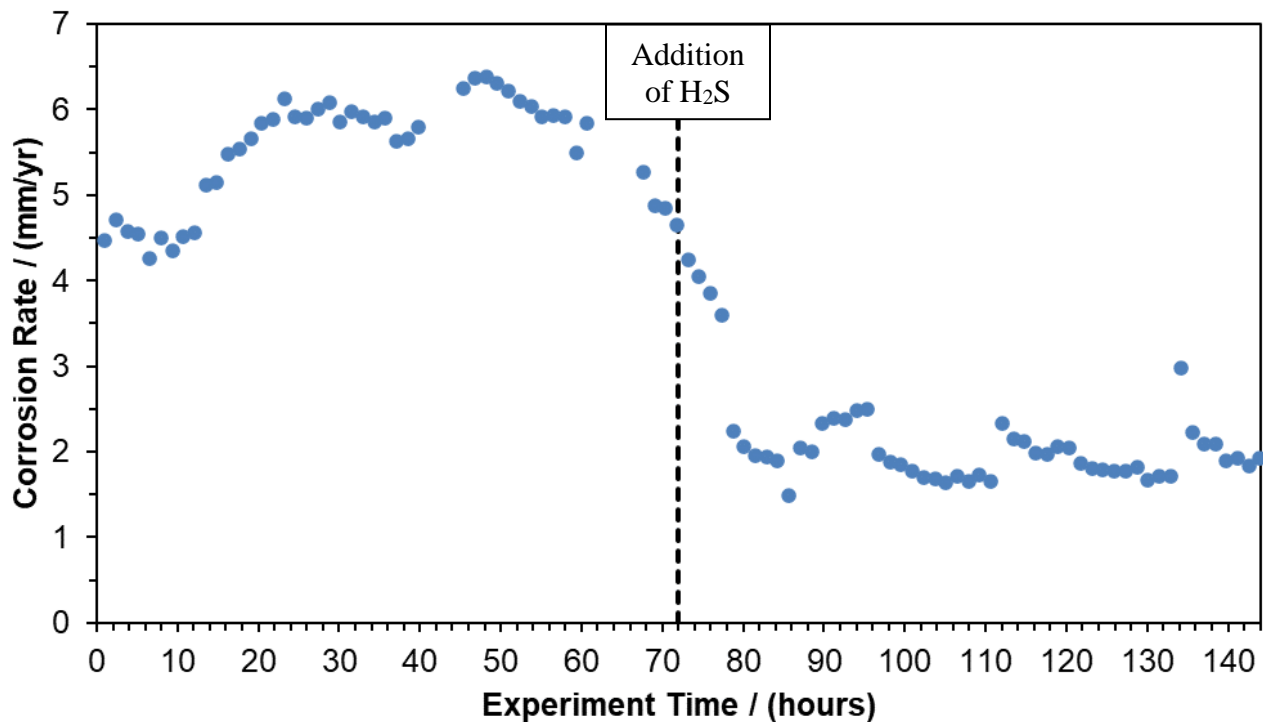


**Figure 4. General corrosion rate vs. time for X65 steel in 1 wt% NaCl solution sparged with pure CO<sub>2</sub> for 72 hours followed by addition of 60 ppm H<sub>2</sub>S in CO<sub>2</sub> for 72 additional hours, 30°C, pH 4.00±0.05, 0.97 bar (14 psi) pCO<sub>2</sub>, ~1 m/s flow.**

In Figure 4 it can be seen that after approximately 24 hours in the pure CO<sub>2</sub> a steady corrosion rate was achieved around 6 mm/yr (236 mpy), the vertical black dashed line represents the point at which H<sub>2</sub>S was introduced into the system. Immediately after the H<sub>2</sub>S was introduced to the system a significant decrease in the general corrosion rate can be seen to around 1.5 mm/yr (59 mpy). To understand this further we can look at the SEM images of the samples extracted before the addition of H<sub>2</sub>S, those extracted after 24 hours exposure to H<sub>2</sub>S, and those extracted at the end of the experiment, seen below in Figure 5, Figure 6, and Figure 7 , respectively.



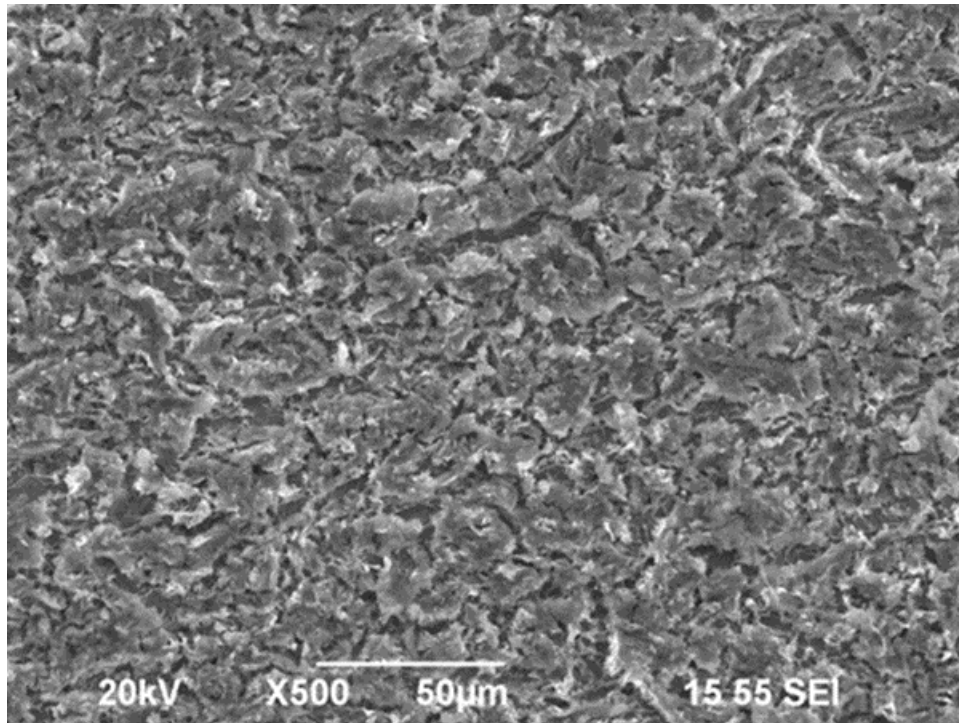


**Figure 5. SEM image of iron carbide present after 72 hours of corrosion in pure CO<sub>2</sub> at 30°C, pH 4.00±0.05, 0.97 bar (14 psi) pCO<sub>2</sub>, ~1 m/s flow.**

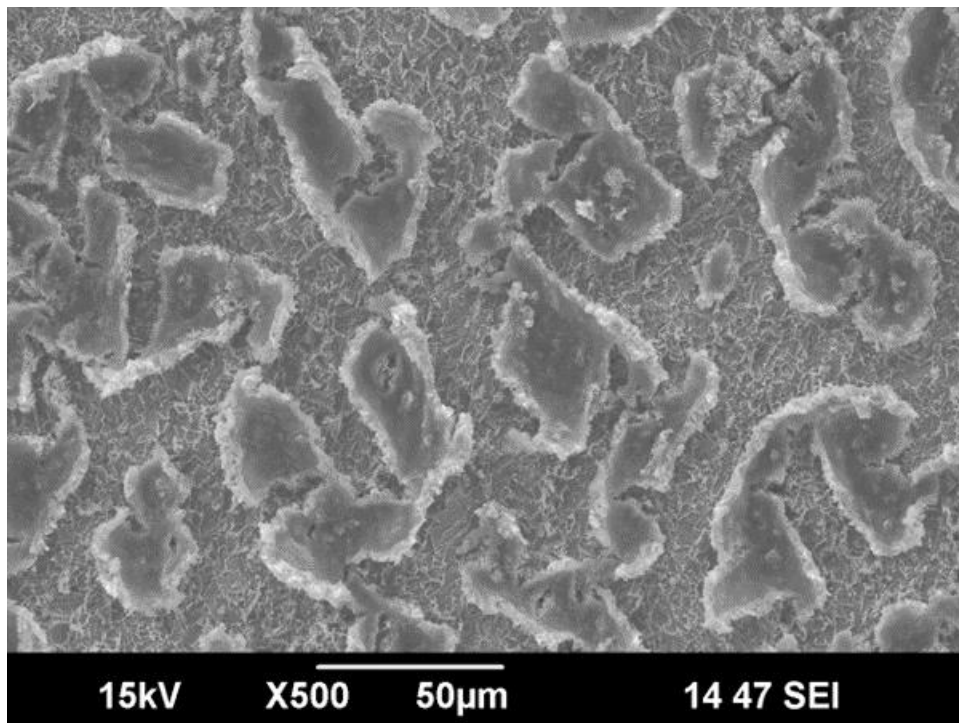


**Figure 6. SEM image of iron carbide with iron sulfide formed after exposure to 60 ppm H<sub>2</sub>S in CO<sub>2</sub> for 24 hours at 30°C, pH 4.00±0.05, 0.97 bar (14 psi) pCO<sub>2</sub>, ~1 m/s flow.**

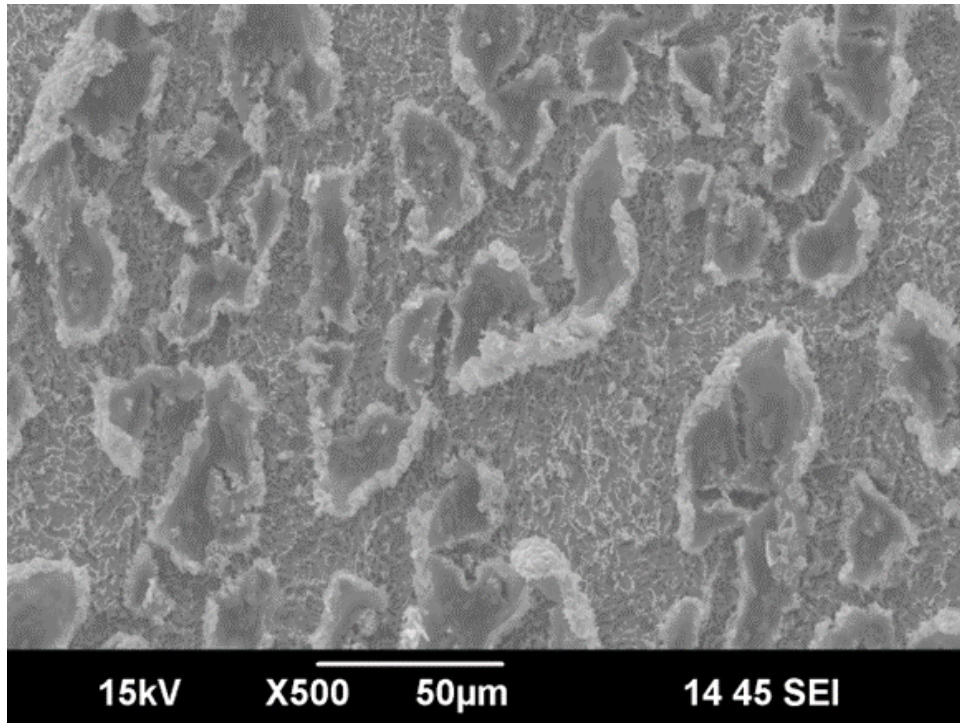


**Figure 7. SEM image of iron carbide layer with iron sulfide formed after exposure to 60 ppm H<sub>2</sub>S in CO<sub>2</sub> for 72 hours at 30°C, pH 4.00±0.05, 0.97 bar (14 psi) pCO<sub>2</sub>, ~1 m/s flow.**

These SEM images show the iron carbide layer had been formed prior to the addition of the H<sub>2</sub>S, and that some of the Fe<sub>3</sub>C layer remained for the duration of the experiment. Further analysis of the layer seen in Figure 7 with EDS mapping shows sulfide species in the surface layer seeming to emphasize the thicker areas where iron carbide layer exists, as shown in Figure 8.

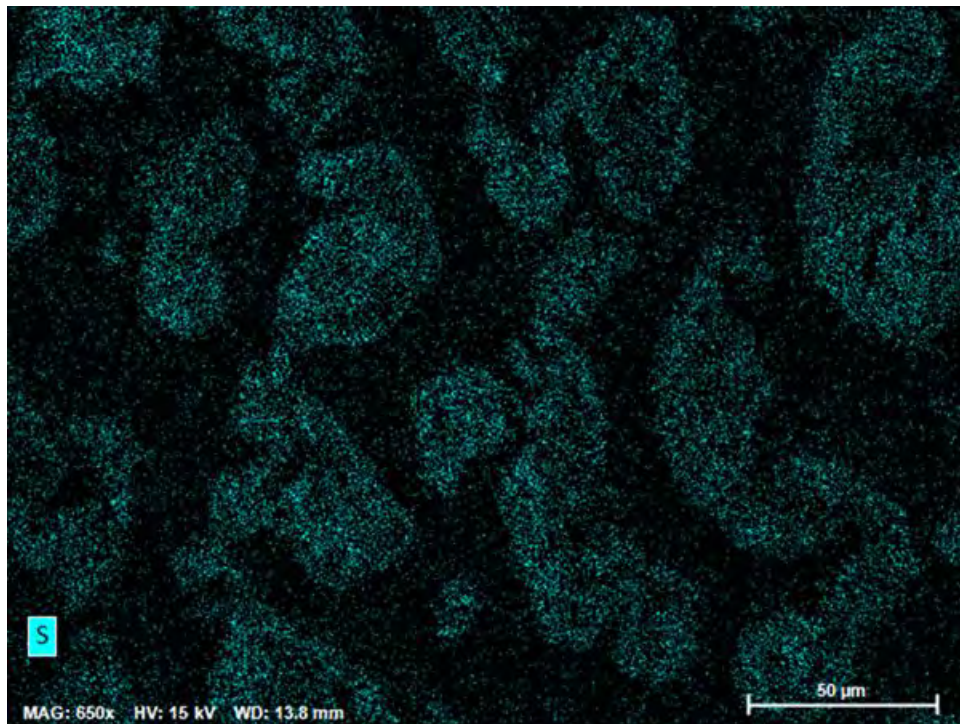


**Figure 8. EDS mapping showing sulfide species in layer formed after exposure to 60 ppm H<sub>2</sub>S in CO<sub>2</sub> for 72 hours at 30°C, pH 4.0±0.05, 0.97 bar (14 psi) pCO<sub>2</sub>, ~1 m/s flow.**



Analysis shows that a sulfide species, likely mackinawite, had formed on the surface of the metal after the addition of the H<sub>2</sub>S which led to the decrease in the general corrosion rate shown in Figure 4. It is unclear how the presence of H<sub>2</sub>S and the formation of an iron sulfide influenced the properties of the iron carbide layer, but the partial loss and deformations in the remaining layer (shown in the previous 3 figures) are not observed in similar experiments without the presence of H<sub>2</sub>S.

### Exposure of an iron carbonate layer (FeCO<sub>3</sub>) to slightly sour environment

Next, similar experiments are performed on an iron carbonate corrosion product layer, the conditions necessary for the formation of iron carbonate can be seen in Table 2. The iron carbonate layer was formed in the presence of pure CO<sub>2</sub> and quiescent flow, additionally the iron ion concentration in the system was artificially increased by the addition of FeCl<sub>2</sub> into the system to give a starting concentration of Fe<sup>2+</sup> of 25 ppm, which corresponds to a super saturation with respect to iron carbonate of 150. After the formation and confirmation of an iron carbonate layer, flow is introduced with the impeller set to 75 rpm (equivalent mass transfer to ~1 m/s flow in a 10 cm ID pipe) and corrosion rate is monitored until it has stabilized, at which point 80 ppm of H<sub>2</sub>S in CO<sub>2</sub> is introduced to the system. Samples are extracted immediately prior the introduction of H<sub>2</sub>S and at the end of the experiment. The general corrosion rate over time in the experiment is shown in Figure 9.

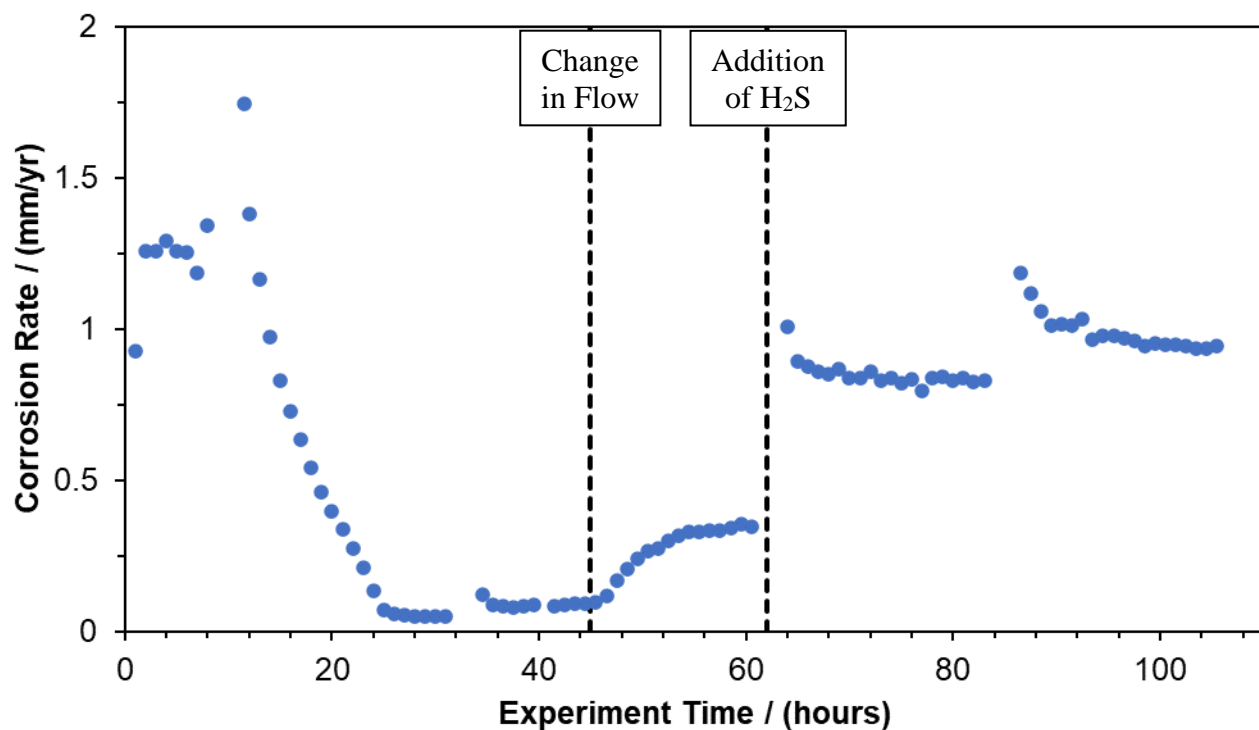


**Figure 9. General corrosion rate vs. time for X65 steel in 1 wt% NaCl solution sparged with pure CO<sub>2</sub> for 48 hours, 17 hours with ~1 m/s flow and CO<sub>2</sub> only, then 80 ppm H<sub>2</sub>S in CO<sub>2</sub> for 66 additional hours, 80°C, pH 6.60, 0.54 bar (7.8 psi) pCO<sub>2</sub>, ~1 m/s flow.**

From the data shown in Figure 9, the corrosion rate had decreased to 0.1 mm/year after 24 hours, indicating that the iron carbonate layer had been successfully formed on the metal surface. When flow was initiated, there was a slight increase in the general corrosion rate. Once the corrosion rate was stable again, 80 ppm H<sub>2</sub>S in CO<sub>2</sub> was introduced to the system. After the introduction of the H<sub>2</sub>S, the corrosion rate immediately increased significantly from 0.25 mm/yr (10 mpy) to 1 mm/yr (39 mpy). To better understand what was occurring, SEM images and EDS analysis of the samples extracted over the course of the experiment are reviewed. Figure 10 and Figure 11 below show SEM images of the samples extracted immediately prior to introduction of the H<sub>2</sub>S, and at the end of the experiment respectively.



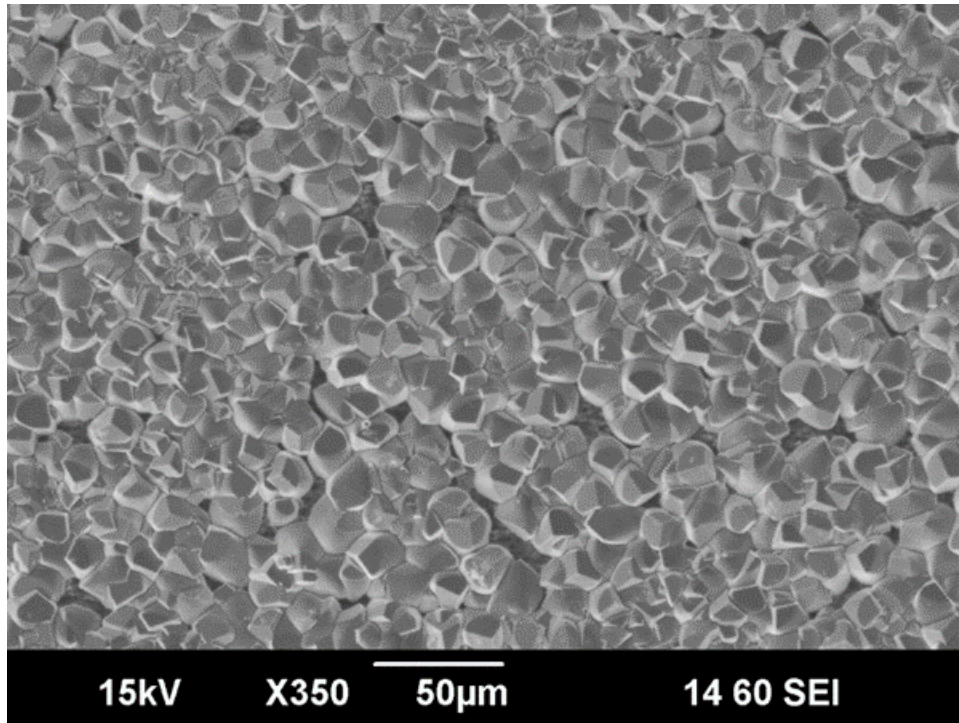


**Figure 10. SEM image of iron carbonate layer after exposure to flow for 12 hours at 80°C, pH 6.6±0.05, 0.54 bar (7.8 psi) pCO<sub>2</sub>, ~1 m/s flow.**

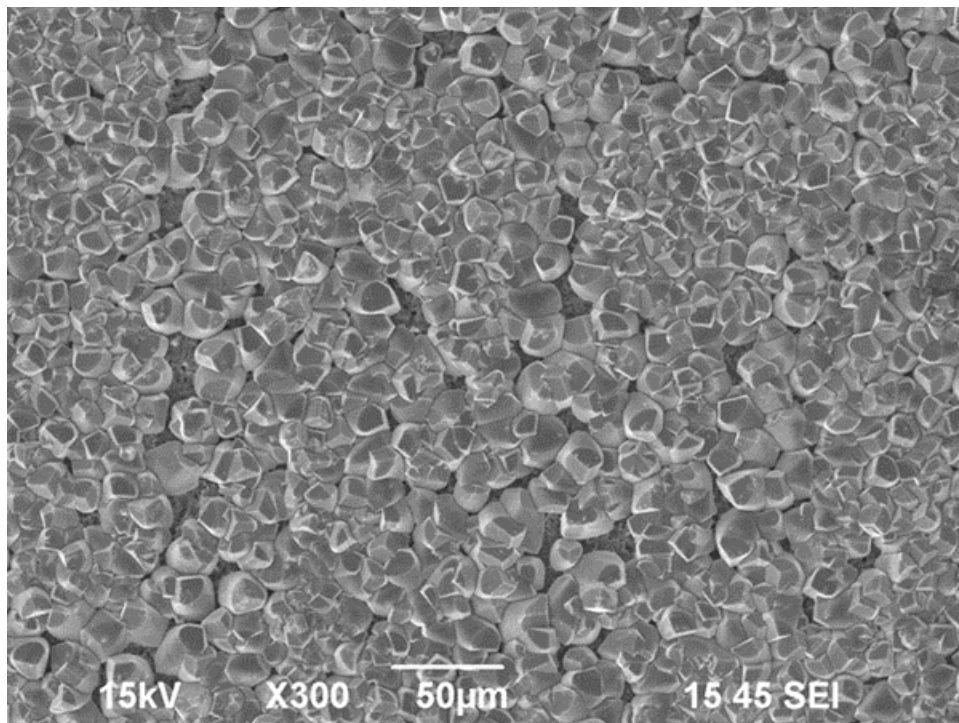


**Figure 11. SEM image of iron carbonate layer after exposure to 80 ppm H<sub>2</sub>S in CO<sub>2</sub> for 62 hours at 80°C, pH 6.6±0.05, 0.54 bar (7.8 psi) pCO<sub>2</sub>, ~1 m/s flow.**

From these images, an iron carbonate layer was present on the metal surface prior to the introduction of the H<sub>2</sub>S, and this iron carbonate layer remained intact after the addition of the H<sub>2</sub>S. In some areas it can be seen that there appears to a substance on the surface of the iron carbonate itself that was not present

prior to the introduction of the H<sub>2</sub>S. EDS analysis of the sample extracted after the exposure to H<sub>2</sub>S shows sulfide species present on the iron carbonate crystals (Figure 12 and Figure 13).

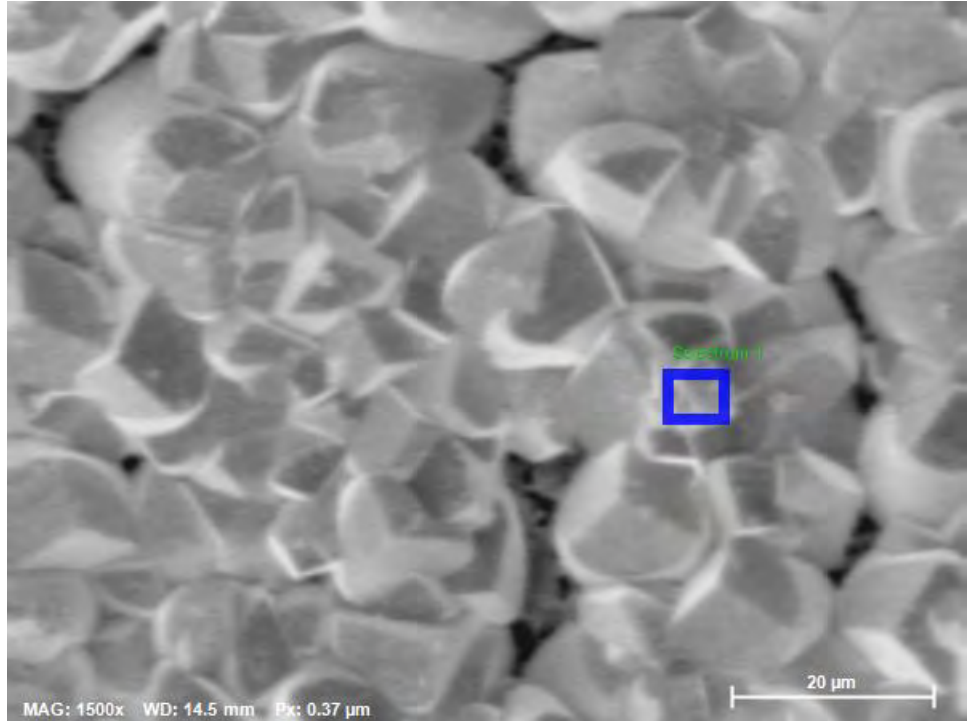


**Figure 12. SEM image being used for EDS analysis of iron carbonate crystals after exposure to 80 ppm H<sub>2</sub>S in CO<sub>2</sub> at 80°C, pH 6.6±0.05, 0.54 bar (7.8 psi) pCO<sub>2</sub>, ~1 m/s flow.**

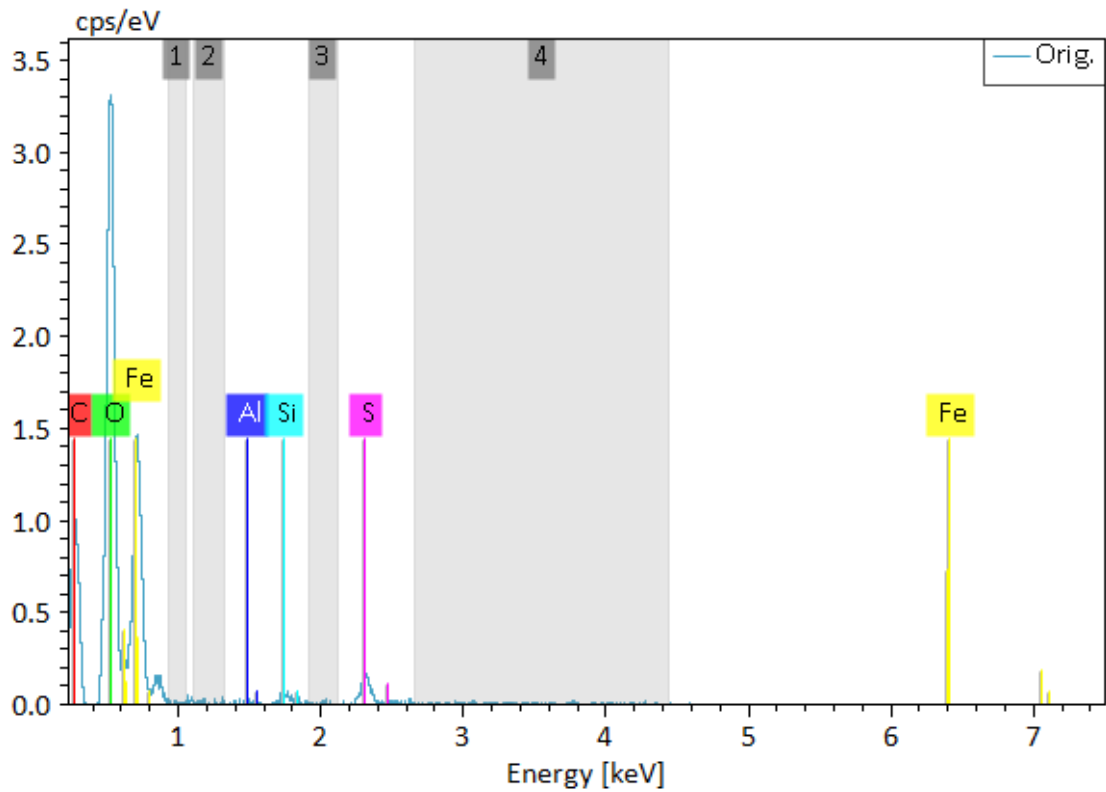


**Figure 13. EDS spectrum of highlighted area shown in Figure 12.**

Sulfide species were also detected in the area between the iron carbonate crystals (metal substrate or iron carbide?) which can be seen in Figure 14 and Figure 15.

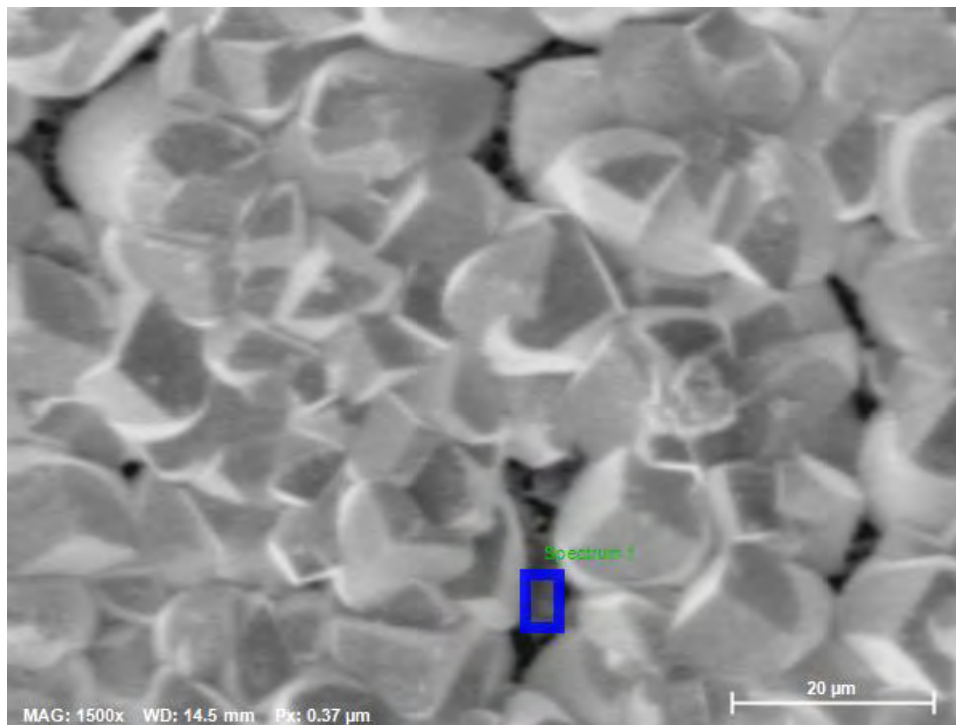


**Figure 14. SEM image being used for EDS analysis of iron carbonate inner layer after exposure to 80 ppm H<sub>2</sub>S in CO<sub>2</sub> at 80°C, pH 6.6±0.05, 0.54 bar (7.8 psi) pCO<sub>2</sub>, ~1 m/s flow.**

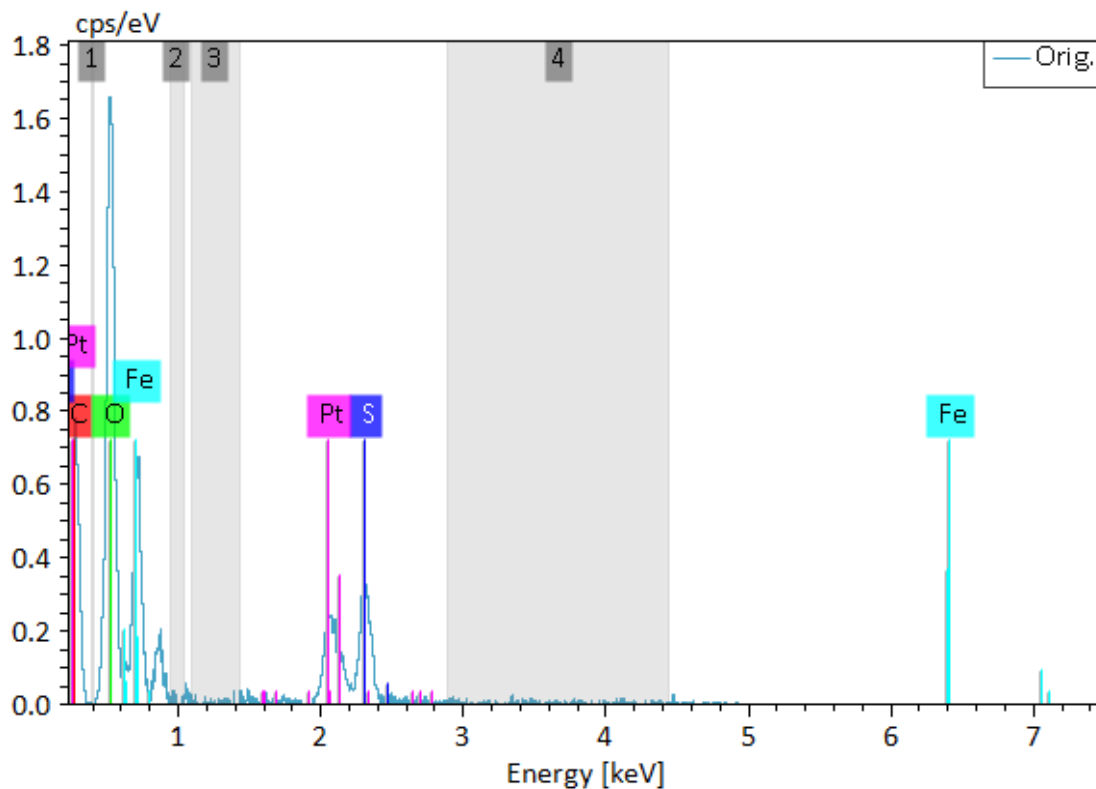


**Figure 15. EDS spectrum of highlighted area shown in Figure 14.**

Comparison of the spectrum peaks for sulfide species seen in Figure 13 and Figure 15 indicate that the sulfide species were present over the entire surface, but are assumed to be more highly concentrated in the gaps between the iron carbonate crystals, though this will require further study.

## CONCLUSIONS

The effect of low concentrations of H<sub>2</sub>S when introduced to existing sweet corrosion product layers was studied using pre-formed iron carbide or iron carbonate layers on an X65 mild steel. When H<sub>2</sub>S was introduced to the iron carbide layer there was a significant decrease in the general corrosion rate. This was likely caused by the formation of an iron sulfide layer which was supported by the EDS analysis. When H<sub>2</sub>S was introduced to the iron carbonate layer there was a significant increase in the general corrosion rate.

- Iron carbide layer remains partially attached after the addition of H<sub>2</sub>S
- Iron sulfide was identified with the iron carbide layer after the introduction of H<sub>2</sub>S
- Iron carbonate layer remains unchanged after exposure to H<sub>2</sub>S
- Iron sulfide was identified with the iron carbonate layer after the introduction of H<sub>2</sub>S

## ACKNOWLEDGEMENTS

The author would like to thank the following companies for their financial support:

Ansys, Baker Hughes, Chevron Energy Technology, Clariant Corporation, ConocoPhillips, ExxonMobil, M-I SWACO (Schlumberger), Multi-Chem (Halliburton), Occidental Oil Company, Pertamina, Saudi Aramco, Shell Global Solutions and TotalEnergies.

## REFERENCES

1. Koch, G.H., M.P.H. Brongers, N.G. Thompson, Y.P. Virmani, and J.H. Payer, "Chapter 1 - Cost of Corrosion in the United States," in *Handb. Environ. Degrad. Mater.*, ed. M. Kutz (Norwich, NY: William Andrew Publishing, 2005), pp. 3–24, <https://www.sciencedirect.com/science/article/pii/B9780815515005500033>.
2. Zheng, Y., "Electrochemical Mechanism and Model of H<sub>2</sub>S Corrosion of Carbon Steel," Ohio University, 2015.
3. Lee, K.-L.J., "A Mechanistic Modeling of CO<sub>2</sub> Corrosion of Mild Steel in the Presence of H<sub>2</sub>S," Ohio University, 2004.
4. Sun, W., "Kinetics of Iron Carbonate and Iron Sulfide Scale Formation in CO<sub>2</sub>/H<sub>2</sub>S Corrosion," Ohio University, 2006.